Design of Mixed Langmuir Films Exposing Segregated Hydroxyl Domains for Inducing Ice Nucleation

Michal Arbel-Haddad, Meir Lahav,* and Leslie Leiserowitz*

Department of Materials and Interfaces, Weizmann Institute of Science, Rehovot 76100, Israel

Received: August 5, 1997

The structure of mixed Langmuir films of the normal alkane $C_{32}H_{66}$ with different quantities of the normal alcohol $C_{31}H_{63}OH$ or the diol $HO(CH_2)_{30}OH$ on pure water were determined in situ by applying surface-sensitive methods that include grazing incidence X-ray diffraction (GIXD) and infrared reflection−absorption spectroscopy (IRRAS) and by induced freezing of water drops. Random solid solutions were formed between the alkane and $C_{31}H_{63}OH$. On the other hand, segregation of the two components was observed in the mixed systems of the alkane and $HO(CH_2)_{30}OH$. These findings suggest new ways for the design of hydrophobic surfaces bearing hydrophilic sites, which may be appropriate for epitaxial ice nucleation and cloud seeding purposes.

Introduction

Although ice melts at 0 °C, pure water droplets may be supercooled to temperatures as low as −40 °C.[1] The process of ice nucleation from supercooled water has attracted a lot of attention over the years, due to its importance in many natural systems. The freezing of supercooled water droplets in rain clouds, for example, is the first step in the process that consequently leads to rainfall. The temperature at which freezing occurs is very much influenced by the chemical and physical nature of particles that are present in the atmosphere and may, or may not, serve as ice nucleation centers. There is a special interest in finding materials that promote ice nucleation at temperatures close to 0 °C, the thermodynamic freezing temperature, for the purpose of cloud seeding. Such materials may allow to induce rainfall from "warm clouds" which are in the temperature range of −8 to 0 °C.

Much of the work in this field had focused on the characterization of materials that promote ice nucleation and the elucidation of their mode of action. The most commonly known artificial ice nucleating material, silver iodide, which induces freezing in rain clouds at −8 °C or lower, was chosen due to the epitaxial match between its crystalline lattice and that of ice.[2] Yet over the years it has been shown that an epitaxial match is only one of the structural features that are important for the nucleation process. The surface properties of a material, and more specifically its ability to bind water from the vapor phase, play a crucial role in determining the ice nucleation efficiency. The importance of surface properties was demonstrated by studies of ice nucleation on silica.[3,4] The ice nucleation activity of amorphous silica particles was reported to increase when its surface was modified to be partially hydrophobic. According to a model proposed by Zettlemoyer, a partially hydrophobic surface leads to the concentration of water molecules at segregated hydrophilic sites, resulting in enhanced ice nucleation efficiency.[5]

Previous studies in our laboratory showed that deposition of alcohols, either *n*-1-alkanols or α,ω-*n*-alkanediols, at the surface of small drops of pure water promotes ice nucleation at temperatures as high as −2 °C.[6−8] The alcohol molecules were found to form two-dimensional crystalline domains at the air−water interface, with a unit cell close to that of the hexagonal form of ice (Figure 1). This packing mode, with a two-dimensional rectangular cell of $a = 5.0$ Å and $b = 7.4$ Å, is typical of many long-chain hydrocarbon molecules.[9] More recently, it was shown that normal alkanes C_nH_{2n+2}, where $n \geq 18$, also form crystalline monolayer and multilayer films at the air−water interface.[10] The structure of these crystalline films is in essence the same as that of their respective three-dimensional crystals and depends on the number of carbon atoms in the molecular chain and whether this number is odd or even. As in the case of three-dimensional crystals, the orthorhombic structure, with the typical orthogonal cell of $a = 5.0$ Å and $b = 7.4$ Å, is obtained in the presence of additives with a similar hydrocarbon chain.

Our goal was to exploit the epitaxial match between this packing mode and the crystalline structure of ice for the design of new ice nucleating materials that are based on long-chain hydrocarbon molecules. The desired surface properties were thought to be attainable by preparing crystalline mixtures of alcohols and alkanes. A surface that resembles the Zettlemoyer model of hydrophilic domains within a hydrophobic matrix will be obtained if the alcohol molecules segregate into domains within a mixed alcohol−alkane layer. Since thin films of the alcohols and those of the alkanes have a similar packing mode and cell dimensions, it seemed reasonable to expect that mixed crystalline films, if formed, will preserve the same intralayer packing arrangement and cell dimensions. The resulting lattice of hydroxyl groups at the hydrophilic domains will retain the epitaxial match with ice.

To test the feasibility of obtaining segregated domains of alcohol molecules within such mixtures, we investigated the miscibility of alcohol−alkane and diol−alkane mixtures at the air−water interface. The mixed films were tested for their ability to induce ice nucleation, and their structure was studied in situ by grazing incidence X-ray diffraction (GIXD) and FTIR spectroscopy.

Experimental Section

Materials. Dotriacontane, $C_{32}H_{66}$ (99% pure), was purchased from Sigma. Its deuterated analogue, d_{66}-dotriacontane, $C_{32}D_{66}$ (98% deuteration), was purchased from Cambridge Isotopes. The preparations of the diol $HO(CH_2)_{30}OH$ (labeled HOC_{30}-

S1089-5647(97)02573-X CCC: $15.00
Published on Web 02/11/1998

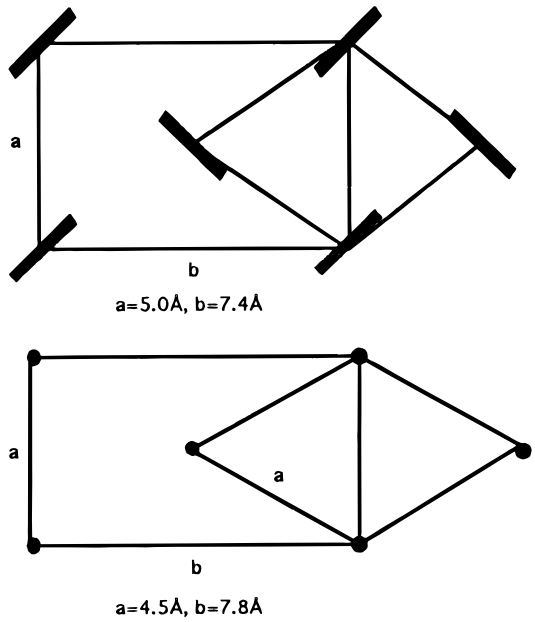

Figure 1. Lattice match between the herringbone packing of hydrocarbon chains (top) and the *ab* lattice of hexagonal ice (bottom).

OH)[6] and alcohol $C_{31}H_{63}OH$ (labeled $C_{31}OH$)[7] were described previously. Spreading solutions for the mixed films were prepared in chloroform (Merck, analytical grade). For preparation of the mixed films, solutions of the two components were premixed to obtain the desired molar ratio and concentration. Millipore purified water was used for the subphase.

Ice Nucleation Experiments. Ice nucleation experiments were carried out in a specially designed chamber described previously.[7] In each experiment, 10−15 water drops, 10 μL each, were placed on a microscope cover glass slide that was pretreated with octadecyltrichlorosilane, yielding a hydrophobic surface. The hydrocarbon film was deposited on the drops at room temperature, by applying 1 μL of a 0.2 mM chloroform solution. In each experiment, at least two of the drops were covered by a pure alcohol film, either $C_{31}OH$ or $HOC_{30}OH$, and at least two were covered by the alkane. These were used as an internal standard.

The glass slides were placed on a copper stage and attached by heat-transfer silicone grease (Unick). A thermoelectric heat pump (Melcor), placed on a cooled copper heat sink, was used for cooling the stage. Cooling rates were approximately 1 °C/min. A stream of cold nitrogen was blown over the sample during the time of the experiment in order to reduce the humidity within the chamber and avoid condensation of additional water drops on the glass plate. Freezing was observed visually, and the temperature at the instance of freezing, as measured by iron−constantan thermocouples attached to the glass slides near the water drops, was recorded.

Grazing Angle X-ray Diffraction. The grazing incidence X-ray diffraction (GIXD) experiments were performed at the undulator BW1 beam line on a liquid surface diffractometer at the Hasylab synchrotron source (Hamburg). A detailed description of the GIXD method was given previously.[11,12]

Mixed films were deposited on the water subphase, so that the calculated coverage is 80%. Deposition was carried out at room temperature. The water subphase was then cooled, and the diffraction pattern was measured at a temperature of ~5 °C.

A monochromated X-ray beam was adjusted to strike the liquid surface at an incident angle $\alpha \approx 0.85\alpha_c$ (where α_c is the critical angle for total external reflection) which maximizes surface sensitivity. The dimensions of the footprint of the incoming X-ray beam on the liquid surface were approximately 5×50 mm^2. GIXD signals are obtained from 2D crystallites azimuthally randomly oriented on the water surface. The scattered intensity was collected by means of a position-sensitive detector (PSD) which intercepts photons over the range $0.0 \leq q_z \leq 0.9$ Å^{-1}, where q_z is the vertical component of the X-ray scattering vector $\approx (2\pi/\lambda) \sin \alpha_f$, α_f being the angle between the horizon and the diffracted beam. Measurements were performed by scanning over a range along the horizontal scattering vector q_{xy} ($\approx 4\pi \sin\theta_{xy}/\lambda$, where $2\theta_{xy}$ is the angle between the incident and diffracted beam projected onto the horizontal plane) and over the whole q_z window of the PSD. The diffraction data are represented in two ways: *Bragg peak intensity profiles* $I(q_{xy})$ are obtained by integrating the whole q_z intensity profile for any q_{xy} along the measured range; *Bragg rod profiles* show the scattered intensity $I(q_z)$ in the channels along the PSD, integrated over the whole range in q_{xy} for a given Bragg peak.

FTIR Measurements. In situ Fourier transform IR measurements of mixed films at the air−water interface were carried out by using a commercial Specac monolayer/grazing angle accessory placed in a Bruker IFS-66 spectrophotometer equipped with a liquid N_2 cooled HgCdTe (MCT) detector. The angle of incidence was 25° from the normal to the surface. Each spectrum was a coaddition of 1000 scans at a 2 cm^{-1} resolution. Reflection−absorption spectra were obtained by taking the ratio of the single-beam monolayer spectrum on water against the single-beam reflectance spectrum of pure water.

Results

Alcohol−Alkane Mixtures. The ice nucleation properties of a series of alcohols $C_nH_{2n+1}OH$ with $n = 13-31$ were previously studied in this laboratory.[8] The freezing temperatures of water drops covered by a monolayer film of the alcohols was found to decrease with decreasing chain length. This was correlated with a decrease in the amount of crystalline material formed, increased molecular motion, and a worse mismatch between the crystalline monolayer film and ice.[13]

It was therefore decided to test the induced ice nucleation temperatures under mixed monolayers composed of the most efficient alcohol in this series, $C_{31}H_{63}OH$ (labeled $C_{31}OH$) and an alkane of comparable length, $C_{32}H_{66}$. The average freezing temperatures induced by these mixtures at various molar ratios are shown in Figure 2. The temperature of ice nucleation was found to decrease with increasing alkane content in the film. This trend was interpreted as indicating the formation of a solid solution, where molecules of the inactive component, $C_{32}H_{66}$, disrupt the lattice of hydroxyl groups at the interface, reducing the coherence of nucleation sites for ice.

Grazing incidence X-ray diffraction was measured for a thin film composed of 50% $C_{31}OH$ and 50% $C_{32}H_{66}$ and for a film of the pure alkane, both at the air−water interface. Six diffraction peaks were observed in the diffraction pattern of the mixed film and were fully indexed in terms of a two-dimensional rectangular unit cell, with dimensions $a = 5.0$ Å and $b = 7.4$ Å (Figure 3a). The diffraction pattern from a film of pure $C_{32}H_{66}$ is similar,[14] yielding essentially the same rectangular two-dimensional unit cell. These 2D cell dimensions are typical of the orthorhombic form of three-dimensional alkane crystals and other long-chain hydrocarbon molecules. The widths of the Bragg peaks along the X-ray scattering vector component q_{xy} for both films are at the instrumental resolution limit and indicate a crystalline coherence length of at least 1000 Å.[15] The

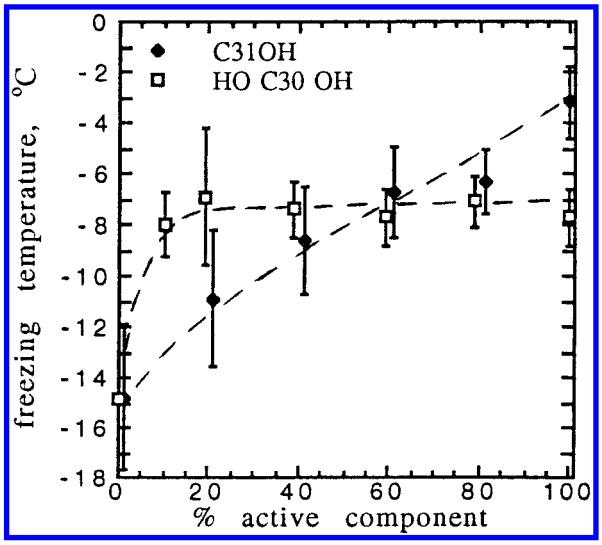

Figure 2. Induced ice nucleation temperatures under mixed films composed of an ice nucleating alcohol, either $C_{31}H_{63}OH$ (rhombs) or $HO(CH_2)_{30}OH$ (squares), and the alkane $C_{32}H_{66}$. Lines were drawn as guides to the eye.

intensity maxima for the (1,1) and (0,2) Bragg rods are close to $q_z = 0$ Å^{-1} (Figure 3b,c), indicating that the molecular chains are essentially perpendicular to the layer plane.[16] The thickness of the films, estimated from the width of the (1,1) and (0,2) Bragg rods, is in the order of 40 Å, which is the length of one fully extended molecule of $C_{31}OH$ and of $C_{32}H_{66}$.[17]

Pure $C_{31}OH$ forms a monolayer film with a two-dimensional unit cell of $a = 5.0$ Å and $b = 7.45$ Å, where the long axis of the molecule is tilted by 9° in the direction of the b axis.[8,18] The direction and angle of the tilt are indicated by the positions of intensity maxima along the (1,1) and (0,2) Bragg rods which are at $q_z \sim 0.15$ Å^{-1} and $q_z \sim 0.30$ Å^{-1}, respectively. It should be noted that these features have been observed in the diffraction pattern of a mixture containing as little as 10% $C_{31}OH$, when the second component was a perfluorinated alcohol which is immiscible with hydrocarbons.[19] Their absence from the diffraction pattern arising from the thin film composed of 50% $C_{31}OH$ and 50% $C_{32}H_{66}$ therefore indicates that a mixed crystalline phase had been formed.

A decrease in ice nucleation temperature with increasing additive content was previously reported for mixtures of $C_{31}OH$ with the alcohols $C_nH_{2n+1}OH$, where $n = 30, 29, 27$.[7] Grazing incidence X-ray diffraction from mixtures of $C_{31}OH$ with $C_{29}OH$ or $C_{27}OH$ confirmed that the alcohols are miscible and form a mixed crystalline monolayer at the air−water interface.[7,18]

Mixtures of $C_{31}OH$ with $C_{32}H_{66}$ do not satisfy the requirements we had set out for domain separation. Although the desired crystalline packing was obtained, the miscibility of the two components leads to the loss of the ice nucleation properties.

Diol−Alkane Mixtures. Several α,ω-diols, $HO(CH_2)_nOH$, $n > 16$, were previously studied in our laboratory and were found to induce ice nucleation at the same temperature range as the corresponding normal alcohols.[6] GIXD studies of the diols at the air−water interface show that they form monolayers and multilayers, yet maintain an intralayer packing motif similar to that of the monofunctional alcohols.[6,20,21]

Mixtures of the diol $HO(CH_2)_{30}OH$, labeled $HOC_{30}OH$, with the alkane $C_{32}H_{66}$ were tested for their ice nucleation efficiency. The length of the diol molecule $HOC_{30}OH$ is comparable to that of the monofunctional alcohol $C_{31}OH$ and alkane. The results are shown in Figure 2, together with those for the alcohol−alkane mixtures. The differences in ice nucleation properties between the two types of mixtures are evident. The nucleation temperatures induced by mixtures of the diol $HOC_{30}OH$ with the alkane $C_{32}H_{66}$ remain constant over a large range of molar ratios in the mixture. The nucleation temperature induced by a mixture containing only 10% diol is close to that of the pure diol. These results are an indication of segregation of the active component, the diol, within the mixed film. The segregated domains of diol molecules serve as active sites for ice nucleation.

Two mixtures, containing 10% or 60% $HOC_{30}OH$, were studied by GIXD. Despite the clear difference in ice nucleation properties, the diffraction data of both mixtures were found to be very similar to that of the alcohol−alkane mixture (Table 1), indicating the formation of a single crystalline phase. The diffraction peaks from both films could be fully indexed in terms of the typical two-dimensional rectangular unit cell, with dimensions $a = 5.0$ Å and $b = 7.4$ Å, the positions of the intensity maxima for the (1,1) and (0,2) Bragg rods for both mixtures indicate that the molecular chains are essentially perpendicular to the layer plane, and the width of the Bragg rods corresponds to a film thickness in the order of 40 Å, which is the length of the fully extended molecules.

The diffraction pattern of pure $HOC_{30}OH$ shows the coexistence of two crystalline phases at the air−water interface.[6] The major phase is a monolayer with a rectangular unit cell of dimensions similar to the alkanes and alcohols; the minor phase is a multilayer, with molecules tilted by about 35° away from the surface normal and interlayer H bonding. The features that correspond to the tilted multilayer structure do not appear in the diffraction pattern of the two mixtures. This may be an indication that alkane molecules have been incorporated into the diol structure, resulting in the inhibition of multilayer formation due to disruption of the interlayer H-bonding motif.

There is an apparent disagreement between the GIXD data and the ice nucleation results for the mixtures of $HOC_{30}OH$ and $C_{32}H_{66}$. The GIXD studies show that the two components are miscible and, moreover, that the structure of the mixed crystalline monolayer is independent of the molar ratio of the two components. Ice nucleation experiments, on the other hand, suggest the existence of segregated domains of diol molecules. FTIR studies were conducted in order to estimate the degree of mixing between the two components within the mixed crystalline films.

Determination of Lateral Order within the Mixed Monolayers Using FTIR Spectra. FTIR spectroscopy was used for probing the lateral distribution of the two mixture components within the mixed monolayers at the air−water interface by applying the method of Snyder et al.[22] In their work FTIR was used for studying the process of phase separation in three-dimensional crystalline mixtures of normal alkanes. The kinetics of the separation process and the size of the growing domains were monitored by following the shape of the scissors bands of methylene groups, which appear at 1468 cm^{-1} for alkanes and similar long-chain hydrocarbons and at 1088 cm^{-1} for their fully deutereated analogues.[22,23] A splitting of these bands into doublets due to intermolecular coupling occurs when the long-chain molecules crystallize in the orthorhombic or monoclinic crystal form, which have two molecules related by glide symmetry in each cell. Due to the short-range nature of such intermolecular interactions, the degree of splitting can be correlated with the number of molecules in the crystalline domain. Coupling occurs only between neighboring hydrocarbon chains that are isotopically alike. This allows the monitor-

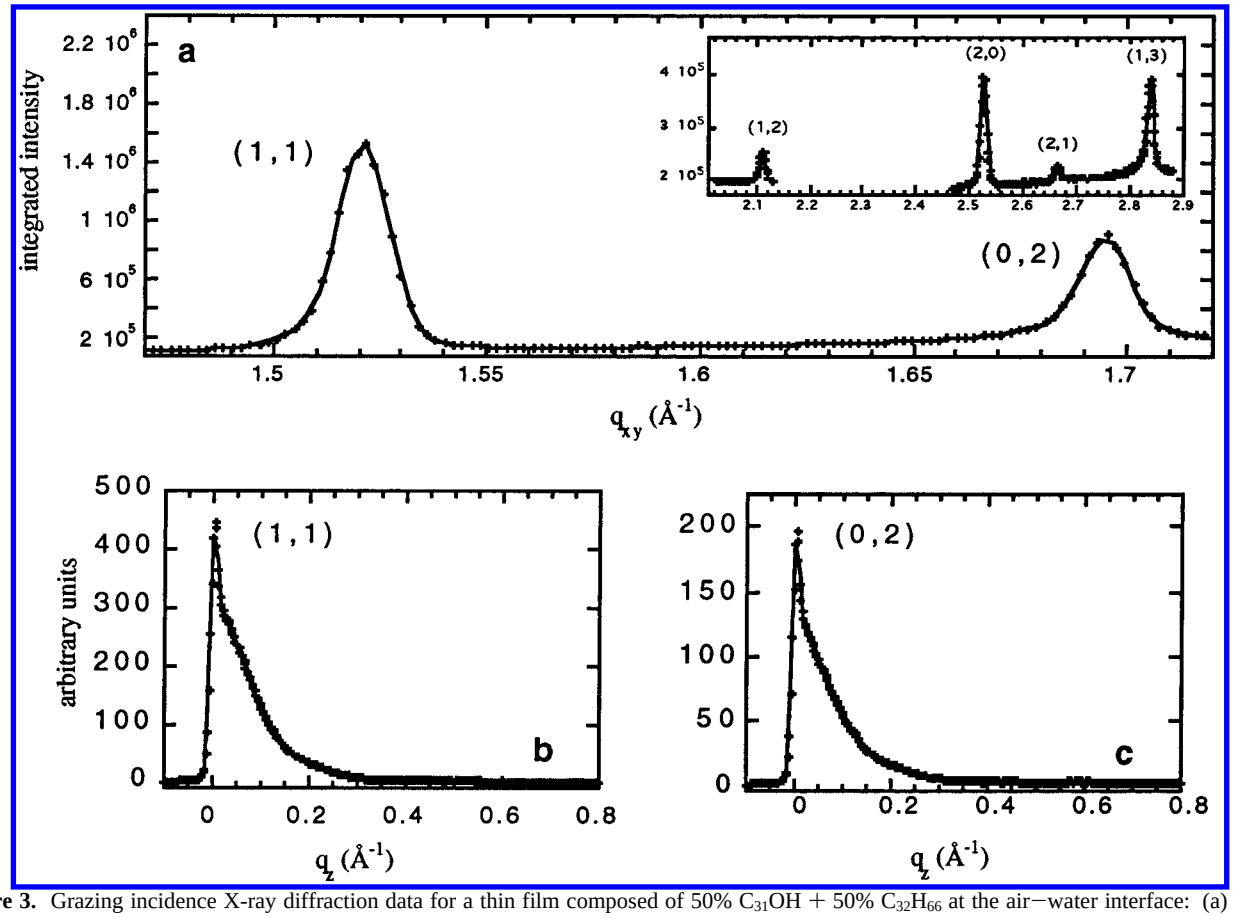

Figure 3. Grazing incidence X-ray diffraction data for a thin film composed of 50% $C_{31}OH$ + 50% $C_{32}H_{66}$ at the air−water interface: (a) Bragg diffraction peaks and (b, c) Bragg rod profiles.

TABLE 1: Positions q_{xy} (top, in Å^{-1}) of the Observed (h,k) Bragg Reflections and Their Relative Integrated Intensities $I(q_{xy})$ (bottom) for the Three Mixed Monolayer Films (0.5:0.5) $C_{31}H_{63}OH$:$C_{32}H_{66}$ and (0.1:0.9) and (0.6:0.4) of $HOC_{30}H_{62}OH$:$C_{32}H_{66}$

(h,k)	50% $C_{31}OH$	10% C_{30} diol	60% C_{30} diol
(1,1)	1.52	1.52	1.52
(0,2)	1.69	1.69	1.69
	0.45	0.52	0.53
(1,2)		2.11	2.11
		0.04	0.05
(2,0)		2.52	
		0.14	
(2,1)		2.66	2.66
		0.03	0.04
(1,3)		2.84	2.84
		0.14	0.21
(2,2)		3.04	
		0.06	

ing of domain size in a two-component mixture composed of a protiated hydrocarbon and a deuterated one.[22]

Our GIXD data showed that the mixed thin films of a mono- or bifunctional alcohol and an alkane crystallize at the air−water interface. Moreover, the two-dimensional unit cell of the mixed thin films was found to be rectangular, with two glide-related molecules per unit cell. It therefore seemed feasible to apply IR spectroscopy to study the distribution of the film components within the crystalline domains.

IR spectra of the mixed films at the air−water interface were measured using the IRRAS (IR reflection−absorption spectroscopy) technique.[24] Some experimental difficulties arose when going from three-dimensional materials to a monolayer at the air−water interface. Absorption of the IR radiation by water vapor prevented the measurement of the CH_2 scissors band at 1468 cm^{-1} in our experimental setup. The CD_2 bands at 1088 cm^{-1} were clearly observed for a wide range of mixture concentrations, yet the signal-to-noise ratio was poor when the deuterated component comprised 20% of the mixture or less.

The mixed films were composed of the long-chain alcohol, $C_{31}OH$ or $HOC_{30}OH$, and a deuterated alkane, $C_{32}D_{66}$. Mixtures of the deuterated alkane $C_{32}D_{66}$ with its protiated analogue $C_{32}H_{66}$ were taken as the standard for a random solid solution. The IR absorption spectra showing the CD_2 scissors band of these mixtures at different mixing ratios are shown in Figure 4a. The IR absorption by mixtures of $C_{31}OH$ and $HOC_{30}OH$ with $C_{32}D_{66}$ in the same region are shown in Figure 4b,c. The data are more conveniently compared when presented in terms of the normalized splitting R, defined as $R = \Delta\nu/\Delta\nu_{max}$, where $\Delta\nu$ is the observed splitting for a given mixture and $\Delta\nu_{max}$ is the splitting for the pure deutereated compound. Figure 5 shows the normalized splitting in the three types of mixtures as a function of composition.

The normalized splitting, R, for mixtures of $C_{32}D_{66}$ in $C_{32}H_{66}$ (Figure 5a), which was taken as a model for a random mixture, decreases linearly with a decrease in the molar ratio of the deuterated component. Similar values were obtained for the normalized splitting in mixtures $C_{31}OH$ with $C_{32}D_{66}$ (Figure 5b). This similarity indicates that $C_{31}OH$ and the alkane are miscible and form randomly distributed solid solutions at the air−water interface, as was indicated by ice nucleation experiments.

The shape of the curve showing the normalized splitting for mixtures of $HOC_{30}OH$ with $C_{32}D_{66}$ (Figure 5c) is distinctly different, showing a plateau over a wide concentration range, with a small decrease only at 40% $C_{32}D_{66}$ content. The deviation from linearity indicates that the diol and alkane are at least partially phase separated, giving rise to domains that

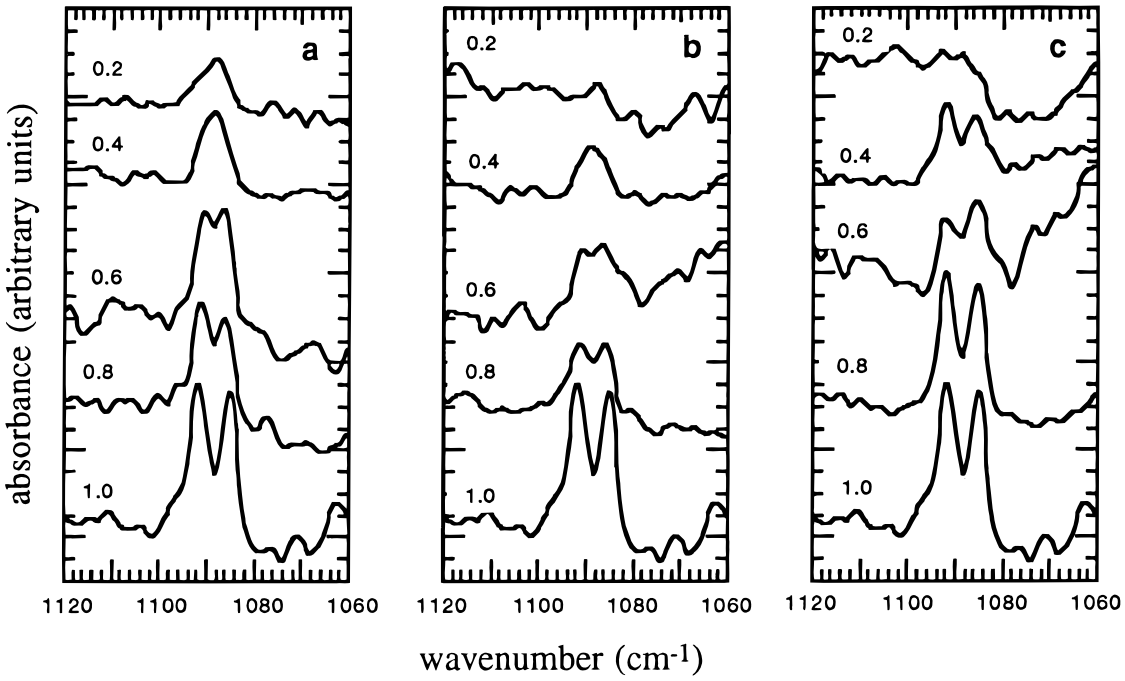

Figure 4. IR spectra showing the region of the CD_2 scissors band for mixtures of $C_{32}D_{66}$ with (a) $C_{32}H_{66}$, (b) $C_{31}OH$, and (c) C_{30} diol. The molar fraction of $C_{32}D_{66}$ in the mixture is noted next to each of the spectra.

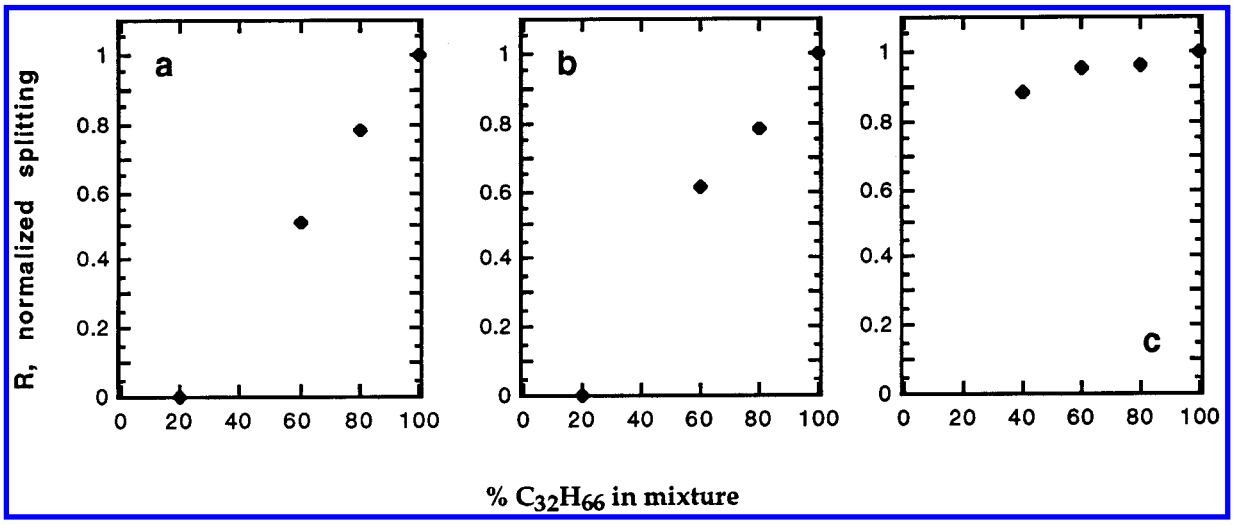

Figure 5. Normalized splitting, R (defined as the ratio Δ/Δ_{max}, where Δ and Δ_{max} are the observed and maximal separation of doublet components), as a function of $C_{32}D_{66}$ content in mixtures with (a) $C_{32}H_{66}$, (b) $C_{31}H_{63}OH$, and (c) $HO(CH_2)_{30}OH$.

are larger than expected for a random solid solution of the same composition. Again, this is in agreement with the results from the ice nucleation experiments.

Discussion

Mixed films of mono- and bifunctional alcohols and alkanes were studied at the air−water interface as part of our project to design surfaces for ice nucleation. Grazing incidence X-ray diffraction (GIXD) enabled the determination of the crystalline structure of the mixed films at the air−water interface. On the basis of these data alone, one may have concluded that the two alcohols, $C_{31}OH$ and $HOC_{30}OH$, are equally miscible in the alkane $C_{32}H_{66}$. Ice nucleation experiments and IR spectroscopy, however, show dramatic differences between mixtures containing the monofunctional alcohol and mixtures containing the α,ω-diol.

Ice nucleation measurements are sensitive to the degree of segregation of the alcohol molecules within the mixed crystalline phase, while FTIR spectra allowed us to probe the degree of aggregation of the alkane molecules. The two techniques are therefore complementary, as can be seen by comparing the results from the two sets of experiments (Figures 2 and 5). Both indicate that $C_{31}OH$ and $C_{32}H_{66}$ form random solid solutions, whereas $HOC_{30}OH$ and $C_{32}H_{66}$ form segregated domains within their mixed films.

The experimental data allow us to get only a rough estimate of the typical aggregate size in the diol−alkane mixtures. The high values of normalized splitting, $R > 0.9$, observed by FTIR for mixtures containing 80% or 60% $C_{32}D_{66}$, can be correlated with coherent alkane domains containing more than 50 molecules.[22] A value of $R = 0.80$, which is correlated with a domain of 20−30 molecules, was obtained for a mixture of 40% $C_{32}D_{66}$ and 60% $HOC_{30}OH$. The diameter of a relatively compact domain of 30 alkane molecules is close to 30 Å. However, the crystalline coherence length obtained by GIXD for a mixed film of the same composition was at least 1000 Å.

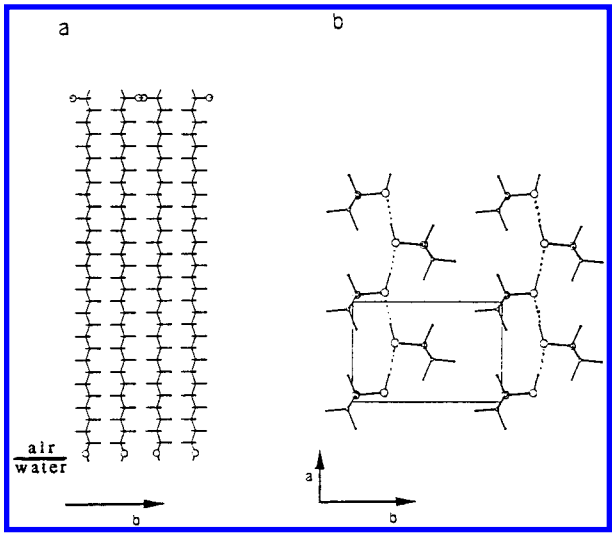

Figure 6. Proposed H-bonding arrangement of OH groups at the interface with air for a monolayer of $HO(CH_2)_{30}OH$ on water. The OH group adopts a gauche conformation about the terminal C−C bond. The O−H···O distance is 2.55 Å along the *a* axis.

The domains of the deuterated alkane molecules must therefore be part of a larger crystalline film.

The efficiency of ice nucleation over a wide range of molar ratios in the diol−alkane mixtures (Figure 2) indicates that the average size of coherent diol domains remains above some critical size which is needed for efficient ice nucleation. Previous X-ray diffraction studies of ice crystals that were nucleated under a monolayer of $C_{31}OH$ led to the conclusion that this critical size is of the order of 30 Å.[25] This is then the estimated minimal size of coherent diol domains within the mixed films containing 20% diol or more.

On the basis of all of these data together, we suggest a model of microphase separation for the mixed thin films containing the diol $HOC_{30}OH$ and an alkane of corresponding length. Segregated domains of the two components, having the same unit cell dimensions, coexist within a crystalline continuum. The size of the segregated diol domains is sufficiently large to allow for efficient ice nucleation even within mixtures containing a large proportion of alkane. Since the only difference between the diol−alkane and alcohol−alkane mixtures is in the presence of a second hydroxyl group in the case of the diol molecules, we suggest that intralayer H bonding by these groups is the driving and stabilizing force for aggregation. Figure 6 shows a possible arrangement of $HO(CH_2)_{30}OH$ molecules interlinked by intralayer H bonding. The molecules adopt a gauche conformation about the C_1-C_2 bond at the interface with air so to achieve intralayer H-bonding.

Microaggregation has been previously reported for three-dimensional crystalline mixtures of alkanes[22] and of methyl esters of fatty acids.[26] It has also been observed in mixtures of phospholipids in the gel state.[26,27] In all the above-mentioned cases the two components of the mixtures differ in the length of the hydrocarbon chain, this difference being the driving force for phase separation. The formation of micro-domains of hydrocarbon chains of the same length had been suggested for mixed monolayers of two thiols with different terminal group on a solid support.[28,29]

We have demonstrated that a separation of territories can be enhanced within a continuous crystalline Langmuir film, while maintaining the desired intralayer packing mode which has proved to be efficient for ice nucleation. We are now investigating the possibility of obtaining similar microaggregated structures in three-dimensional crystals, in order to investigate their activity as promoters of ice nucleation for cloud-seeding purposes.

Acknowledgment. Grazing incidence X-ray diffraction experiments were conducted in collaboration with K. Kjær form the Department of Solid State Physics, Risø National Laboratory, Denmark, and J. Als-Nielsen from the Niels Bohr Institute, Denmark, at the BW1 beamline at HASYLAB, Hamburg. We thank the USA/Binational Foundation for financial support and are grateful to HASYLAB, Hamburg, for synchotron beam time.

References and Notes

(1) Kuhns, I. E.; Mason, B. J. *Proc. R. Soc. London A* **1968**, *302*, 437.
(2) Vonnegut, B. *J. Appl. Phys.* **1947**, *18*, 593.
(3) Basset, D. R.; Boucher, E. A.; Zettlemoyer, A. C. *J. Colloid Interface Sci.* **1970**, *34*, 436.
(4) Salazar, I.; Sepúldeva, L. *J. Colloid Interface Sci.***1983**, *94*, 70.
(5) Tcheurekdjian, N.; Zettlemoyer, A. C.; Chessick, J. J. *J. Phys. Chem.* **1964**, *68*, 773.
(6) Popovitz-Biro, R.; Edgar, R.; Majewski, J.; Cohen, S.; Margulis, L.; Kjær, K.; Als-Nielsen, J.; Leiserowitz, L.; Lahav, M. *Croat. Chem. Acta* **1996**, *69*.
(7) Popovitz-Biro, R.; Wang, J.-L.; Majewski, J.; Shavit, E.; Leiserowitz, L.; Lahav, M. *J. Am. Chem. Soc.* **1994**, *116*, 1179.
(8) Gavish, M.; Popovitz-Biro, R.; Lahav, M.; Leiserowitz, L. *Science* **1990**, *250*, 973.
(9) Small, D. M. *The Physical Chemistry of Lipids Handbook of Lipid Research*; Plenum Press: New York, 1986; Vol. 4.
(10) Weinbach, S. P.; Weissbuch, I.; Kjaer, K.; Bouwman, W. G.; Als-Nielsen, J.; Lahav, M.; Leiserowitz, L. *Adv. Mater.* **1995**, *7*, 857.
(11) Als-Nielsen, J.; Kjaer, K. In *Proceedings of the Nato Advanced Study Institute, Phase Transitions in Soft Condensed Matter;* Riste, T., Sherrington, D., Eds.; Plenum Press: New York, 1989; p 113.
(12) Jacquemain, D.; Grayer Wolf, S.; Leveiller, F.; Deutsch, M.; Kjaer, K.; Als-Nielsen, J.; Lahav, M.; Leiserowitz, L. *Angew. Chem., Int. Ed. Engl.* **1992**, *31*, 130.
(13) Majewski, J. Ph.D. Thesis, Weizmann Institute of Science, 1995.
(14) Seven diffraction peaks were observed at q_{xy} values of 1.525, 1.695, 2.115, 2.53, 2.67, 2.84, and 3.045 $Å^{-1}$ and were indexed as the (1,1), (0,2), (1,2), (2,0), (2,1), (1,3), and (2,2) reflections of a 2D rectangular unit cell with dimensions $a = 5.0$ Å and $b = 7.45$ Å.
(15) The full width at half-maximum (fwhm) of the Bragg peaks in q_{xy} units yields the two-dimensional crystalline coherence length, *L*, associated with the (*h*,*k*) reflection, according to the Scherrer formula: $L = 0.9(2\Pi)/(\text{fwhm})^2 - \Delta^2)^{1/2}$. Δ is the minimal width of the peak, determined by the resolution of the Soller collimator in the experimental setup.
(16) The intensity of a particular value of q_z in a Bragg rod is determined by the square of the molecular structure factor $|F_{hk}(q_z)|$.[2] The position of the maximum of this profile, q_z^0, is related to *t*, the angle between the long axis of the chain molecule and the surface normal: $\cos(\chi_{hk}) \tan t = q_z^0/|\mathbf{q}_{hk}|$. χ_{hk} is the azimuthal angle between the tilt direction projected on the *xy* plane and the reciprocal vector $\mathbf{q}_{hk}$.
(17) The full width at half-maximum of the Bragg rod profile, Δq_z, gives a measure of the thickness of the crystalline film $= 0.9(2\Pi)/\Delta q_z$.
(18) Wang, J. L. Ph.D. Thesis, Weizmann Institue of Science, 1992.
(19) Majewski, J.; Popovitz-Biro, R.; Edgar, R.; Arbel-Haddad, M.; Kjær, K.; Bouwman, W.; Als-Nielsen, J.; Lahav, M.; Leiserowitz, L. *J. Phys. Chem. B* **1997**, *101*, 8874.
(20) Popovitz-Biro, R.; Majewski, J.; Margulis, L.; Cohen, S.; Leiserowitz, L.; Lahav, M. *J. Phys. Chem.* **1994**, *98*, 4970.
(21) Majewski, J.; Edgar, R.; Popovitz-Biro, R.; Kjaer, K.; Bouwman, W. G.; Als-Nielen, J.; Lahav, M.; Leiserowitz, L. *Angew. Chem., Int. Ed. Engl.* **1995**, *34*, 649.
(22) Snyder, R. G.; Goh, M. C.; Srivatsavoy, V. J. P.; Strauss, H. L.; Dorset, D. L. *J. Phys. Chem.* **1992**, *96*, 10008.
(23) Snyder, R. G. *J. Mol. Spectrosc.* **1961**, *7*, 116.
(24) Mendelsohn, R.; Brauner, J. W.; Gericke, A. *Annu. Rev. Phys. Chem.* **1995**, *46*, 305.
(25) Majewski, J.; Popovitz-Biro, R.; Kjaer, K.; Als-Nielsen, J.; Lahav, M.; Leiserowitz, L. *J. Phys. Chem.* **1994**, *98*, 4087.
(26) Snyder, R. G.; Strauss, H. L.; Cates, D. A. *J. Phys. Chem.* **1995**, *99*, 8432.
(27) Mendelsohn, R.; Liang, G. L.; Strauss, H. L.; Snyder, R. G. *Biophys. J.* **1995**, *69*, 1987.
(28) Bain, C. D.; Evall, J.; Whitesides, G. M. *J. Am. Chem. Soc.* **1989**, *111*, 7155.
(29) Stranick, S. J.; Parikh, A. N.; Tao, Y. T.; Allara, D. L.; Weiss, P. S. *J. Phys. Chem.* **1994**, *98*, 7636.